Journal of
Ship&Ocean
Technology
©MARCH 2007

SOTECH Vol. 11, No. 1, pp. 11 ~ 24, 2007

Prediction of Ship Manoeuvrability in Initial Design Stage Using CFD Based Calculation

Yu Rim Cho[1], Bum Sang Yoon[2], Deuk Joon Yum[2] and Myen Sik Lee[3]

[1] Dept. of Naval Architecture & Ocean Engineering, Univ. of Ulsan, Ulsan, Korea
[2] Dept. of Naval Architecture & Ocean Engineering, Univ. of Ulsan, Ulsan, Korea
[3] Hyundai Mipo Dockyard, Ulsan, Korea;
Corresponding Author: bsyoon@ulsan.ac.kr

Abstract

Better prediction of a ship's manouevrabilty in initial design stage is becoming more important as IMO manoeuvring criteria has been activated in the year of 2004. In the present study, in order to obtain more exact and reliable results for ship manoeuvrability in the initial design stage, numerical simulation is carried out by use of RANS equation based calculation of hydrodynamic forces exerted upon the ship hull. Other forces such as rudder force and propeller force are estimated by one of the empirical models recommended by MMG Group. Calculated hydrodynamic force coefficients are compared with those obtained by empirical models. Standard manoeuvring simulations such as turning circle and zig-zag are also carried out for a medium size Product Carrier and the results are compared with those of pure empirical models and manoeuvring sea trial.

Generally good qualitative agreement is obtained in hydrodynamic forces due to steady oblique motion and steady turning motion between the results of CFD calculation and those of MMG model, which is based on empirical formulas. The results of standard manoeuvring simulation also show good agreement with sea trial results.

Keywords: manoeuvrability, FLUENT, hydrodynamic forces, CFD, MMG model, product Carrier

1 Introduction

Evaluation of ship manoeuvrability in initial design stage is becoming more important factor as IMO manoeuvring criteria "(IMO 2002)" has been activated to all ships constructed on or after 1 January 2004. So far, MMG model "(Inoue et al 1981, Kijima et al 1990 and Takashina and Ishiguro 1993)" has been most frequently used for the simulation of ship manoeuvrability in initial design stage. In MMG model, relevant hydrodynamic coefficients are expressed as very simple regression formulas obtained from large variety of experimental data. In order to ensure enough accuracy of the manoeuvring simulation, accurate prediction of hydrodynamic forces, which are combined effects of ship hull, rudder and propeller, are necessary. However, accuracy of the simulation seems to be open to question whenever we confirm large differences between the simulated results and those of sea trial. Lack of experimental data for the same ship type and uncertainties related to scale effects and

environmental conditions during sea trial, etc are the ones of the reasons.

Even though more accurate manoeuvring prediction can be made by captive model test with a planar motion mechanism (PMM), it requires special facilities and more time and cost than using simple regression formulas based on experimental and empirical data.

Recent advancements in computational fluids dynamics (CFD) enable application of Reynolds-Averaged Navier-Stokes (RANS) equation to the prediction of viscous flow around and forces to manoeuvring ship "(Ohmori and Miyata 1993, Fujino 1996, Kim and Kim 2001, Tahara et al 2002 and Lee et al 2004)". It is quite challengeable to apply CFD technique to the flow problems due to ship manoeuvring motions from the following reasons.

① Hydrodynamic forces acting on the ship hull by manoeuvring motions are mainly due to fluid viscosity
② Mostly, in obtaining ship manoeuvring hydrodynamic forces, lots of cost ineffective PMM experiments are to be performed.
③ Recent advancements in CFD technique, computation time, memory size and pre/post processors make the application of RANS solver to the present problems more plausible.

In the present paper, applicability of CFD technique for the prediction of manoeuvring hydrodynamic forces and moments in oblique advancing and steady turning of barehull is investigated. Various hydrodynamic coefficients due to barehull motion are obtained from the CFD results of hydrodynamic forces and moments. For the CFD calculation, well-known and actively verified commercial RANS solver FLUENT "(FLUENT 2003)" is used.

Hydrodynamic coefficients obtained from RANS solver are compared with those of empirical formulas based on MMG models suggested by Inoue et al (1981) and Kijima et al (1990). Inoue's model is used for the linear hull related hydrodynamic coefficients and Kijima's model is used for the rest of hydrodynamic coefficients. Besides, manoeuvring simulations of 35° degree turning and 10°/10° and 20°/20° zig-zag manouevres are carried out to compare with those of MMG model and actual sea trial. All the above analysis was carried out for a medium size Product Carrier.

2 Mathematical models

As shown in Figure1, ship fixed right handed coordinate system is used with the origin on the undisturbed free surface, x and y axes on the horizontal plane, and z axis directed vertically downward.

Employing above mentioned MMG models, equations of ship manoeuvring motions in horizontal plane, surge-sway-yaw, are expressed as follows:

$$m'(\dot{u}' - v'r') = X'_H + X'_P + X'_R \tag{1}$$

$$m'(\dot{v}' + u'r') = Y'_H + Y'_P + Y'_R \tag{2}$$

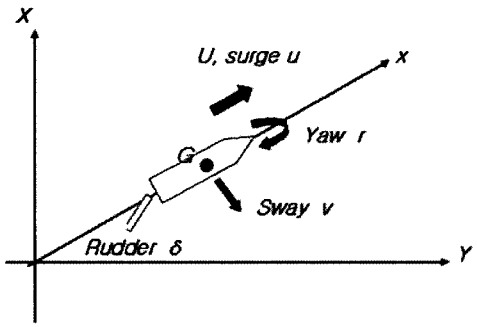

Figure1: Coordinate system

$$I'_{zz}\dot{r}' = N'_H + N'_P + N'_R \tag{3}$$

where m', I'_{zz} are non-dimensional values of ship mass and mass moment of inertia about z-axis, respectively.
Subscripts *H, P* and *R* in the right hand side of the equations denote hull, propeller and rudder forces resulting from ship manoeuvring motions. As shown in the equations of motions, the forces consist of the individual open water characteristics of hull, propeller and rudder and the interaction effects between them. Among the various equation models for the hydrodynamic forces due to barehull only, X'_H, Y'_H, N'_H, following mathematical model is used for the present study.

$$X_H = X_{\dot{u}}\dot{u} + X_{vr}vr + X_{uu}u^2 \tag{4}$$

$$Y_H = Y_{\dot{v}}\dot{v} + Y_v v + Y_{\dot{r}}\dot{r} + Y_{ur}ur + Y_{vv}|v|v + Y_{vr}|r|v + Y_{rr}|r|r \tag{5}$$

$$N_H = N_{\dot{v}}\dot{v} + N_{\dot{r}}\dot{r} + N_v v + N_r r + N_{vv}|v|v + N_{rr}|r|r + N_{vvr}v^2 r + N_{vrr}vr^2 \tag{6}$$

Variables are non-dimensionalized as follows:

$$\left(m', m'_x, m'_y\right) = \left(m, m_x, m_y\right) \Big/ \frac{1}{2}\rho L^2 d \tag{7}$$

$$\left(I'_{zz}, J'_{zz}\right) = \left(I_{zz}, J_{zz}\right) \Big/ \frac{1}{2}\rho L^4 d \tag{8}$$

$$\left(u', v'\right) = \left(u, v\right)/U \tag{9}$$

$$r' = r \cdot \left(\frac{L}{U}\right) \tag{10}$$

$$\left(X', Y'\right) = \left(X, Y\right) \Big/ \frac{1}{2}\rho L d U^2 \tag{11}$$

$$N' = N \Big/ \frac{1}{2}\rho L^2 d U^2 \tag{12}$$

where, ρ, *L, d,* and *U* are water density, ship length, draft and ship's advance speed, respectively.

Hydrodynamic coefficients in equations (4~6) are expressed in terms of the ship's principal dimensions as follows. Linear coefficients are adopted from Inoue et al (1981) and nonlinear ones from Kijima(1990).

$$X'_{\dot{u}} = -m'_x = m' - Y'_r - 1.5C_B B/L \cong (0.1 \sim 0.3)m' \tag{13}$$

$$X'_{vr} = -1.6375C_B Y'_{\dot{v}} + 1.48Y'_{\dot{v}} \tag{14}$$

$$X'_{uu} = (1+kk)C_F, \text{ from Schoenherr Formula} \tag{15}$$

where, $kk = 0.7253 - 2.3225C_B + 2.1437C_B^2$

$$Y'_{\dot{v}} = -m'_y = -\pi/2 \cdot k\{1 + 0.16C_B B/d - 5.1(B/L)^2\} \tag{16}$$

where, $k = 2d/L$

$$Y'_v = -\pi/2 \cdot k - 1.4C_B B/L \tag{17}$$

$$Y'_r = \pi/4 \cdot k \tag{18}$$

$$Y'_{vr} = -5.95d(1-C_B)/B \tag{19}$$

$$Y'_{vv} = -2.5d(1-C_B)/B - 0.5 \tag{20}$$

$$Y'_{rr} = 0.343dC_B/B - 0.07 \tag{21}$$

$$N'_{\dot{r}} = -J'_{zz} = \pi/2 \cdot k\{1/12 + 0.07C_B B/d - 0.33B/L\} \tag{22}$$

$$N'_v = -k \tag{23}$$

$$N'_r = -0.54k + k^2 \tag{24}$$

$$N'_{vv} = 0.96d(1-C_B)/B - 0.066 \tag{25}$$

$$N'_{rr} = 0.5C_B B/L - 0.09 \tag{26}$$

$$N'_{vvr} = -\{57.5(C_B B/L)^2 - 18.4C_B B/L + 1.6\} \tag{27}$$

$$N'_{vrr} = 0.5dC_B/B - 0.05 \tag{28}$$

Semi-empirical models for propeller forces (X'_P, Y'_P, N'_P) and rudder forces (X'_R, Y'_R, N'_R) are also adopted from Kijima et al (1990) and details can be referred to the original paper.

3 Method of viscous calculations

The governing equations of the fluid motion are RANS equation and the incompressible continuity equation. For the present study, commercial RANS solver FLUENT is used. FLUENT is finite-volume type well-known RANS solver and has been fully verified in many research papers related to ship hydrodynamic problems as giving fairly accurate numerical solutions, especially for unsteady free surface problems. Starting with ship

offset data, ship surface shape modeling is carried out using CATIA. Fluid domain is discretized into block-structured grid system utilizing multi-block domain decomposition technique to cope with complex hull form at bulbous bow and stern. GRIDGEN, which is commercial grid generation program, is used. Computational grid system configuration for medium size Product Carrier is shown in Figure2. Simply H-O type grid system is used for the convenience of representing the free surface and interior domain around typical U-shaped hull form, respectively. Computational domain, accepted to be appropriate for the present calculation from preliminary case study, is as follows:

$$-2.5L \le x \le 2.0L, \quad -1.5L \le y \le 1.5L, \quad 0 \le z \le 1.5L$$

Due to the asymmetric flow phenomenon considered, both sides of the ship have to be discretized, doubling the usual number of cells and increasing the computing times compared to straight ahead ship motion. The whole grid system consists of 5 blocks including three blocks numbered in Figure 2 and one block each at bow and stern parts of the vessel, respectively. The number of grids used for the present study was about 478,000 altogether in most of the cases. The minimum grid size on the hull surface was determined based on the criteria that average wall y+ value to be maintained below 100.

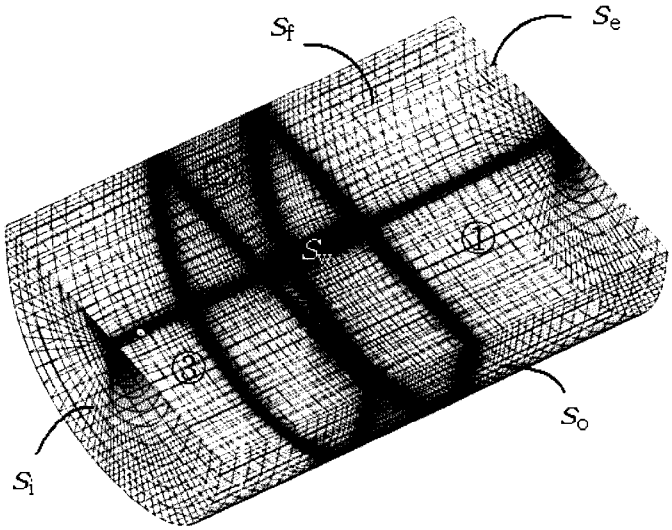

Figure2: Configuration of grid system

The computational method solves the steady RANS and incompressible continuity equations for mean velocity components, *(u, v, w)* and piezometric pressure *P* using the coupled and implicit scheme. The RNG (Renormalization Group) k-ε turbulent model is employed in order to consider flow turbulence. Convection terms in the mass and momentum transport equations are approximated with 2nd order upwind scheme, and diffusion terms with the central differencing scheme. QUICK scheme is used for the convection of turbulence kinetic energy and turbulence dissipation rate.

It is quite straightforward to use the inertial reference frame (non-accelerating frame) for the modeling of oblique steady motions of the vessel. Referring to Figure 2, boundary

conditions applied for each boundary are velocity inlet boundary condition for the inlet plane s_i, pressure outlet boundary condition for the exit plane s_e and the outer boundary s_o and no slip condition with standard wall function at the wall surface s_w. Inflow velocities are input for the velocity inlet boundary condition. The pressure outlet boundary condition is applied for the boundary when the flow velocities on the boundary need to be determined as a solution. The static pressure, which is set to zero in our case, is given as input for the pressure outlet boundary condition.

Because of the relatively low Froude number, $F_n = 0.179$, the free surface is not expected to have a significant influence on the measured forces for moderate drift angles and turning rates. Therefore, free surface, s_f is assumed to be rigid symmetry plane.

But in order to model steady turning motions, the rotating reference frame (accelerating reference frame) option of FLUENT need to be used. The rotating boundary, which is the boundary of steady turning vessel in our study, becomes stationary relative to the rotating frame, since it is moving at the same speed as the rotating reference frame. The pressure inlet boundary condition is used for the boundaries when the inflow velocities are unknown beforehand. And the pressure outlet boundary condition is applied for the boundaries when the outflow velocities are unknown beforehand. Therefore, these boundary conditions are assigned to the boundaries depending on the types of vessel motion (Fluent (2003)). The other boundary conditions are same to the cases of steady oblique motions.

The equations are transformed from Cartesian coordinates in the physical domain into boundary fitted, non-orthogonal, curvilinear coordinates in the computational domain.

4 Review of numerical analysis

4.1 Analysis condition

Computations are carried out for a 6.504 m (scale:26.754) model of medium size Product Carrier at Reynolds number R_n = 8.826*10^6 and Froude number F_n = 0.179 in steady oblique motion as well as steady turning motion with constant speed and zero drift angle. Center of turning motion is located at the longitudinal center of buoyancy. Table 1 shows the principal dimensions of the vessel at design draft of 11m in full scale. Table 2 and Table 3 show CFD calculation conditions for steady oblique motion and steady turning, respectively.

4.2 Numerical results and comparison

A specific history of computation convergence is shown in Figure3. Even though most difficult case is taken, steady turning with forward speed for example, about 1000 iterations are quite enough to obtain fully converged solutions, that is, variation of fluid mass, momentum and turbulence related scale residuals to about 10^{-4} and satisfying degree of convergence of the hydrodynamic coefficients. It takes about 2 hours using Pentium IV equivalent PC. After above convergence criteria is fully satisfied, very small oscillation in the computed hydrodynamic force is noticed. The magnitude of this oscillation was too small to influence the solution accuracy for our study. But the origin of this oscillation would be a topic of further study.

Table 1: Principal dimensions of medium size PC (scale: 26.754)

Ship Type	Product Carrier
LBP(m)	6.5037
Breadth (m)	1.2036
Draft(m)	0.4112
C_B	0.79
LCB (fwd.+)(m)	0.0972
Speed (m/s)	1.442
F_n	0.179
R_n	8.826 e06
Bulb Type	High
Bulb Length (m)	5.0 (Fwd. FP)

Table 2: Conditions for steady oblique motion

β(deg.)	1	2	3	6	9
v(m/s)	0.025	0.05	0.0755	0.151	0.226
v'	0.0175	0.0349	0.0523	0.105	0.156
β(deg.)	12	16	20	25	30
v(m/s)	0.3	0.397	0.493	0.609	0.721
v'	0.208	0.276	0.342	0.426	0.5

Table 3: Conditions for steady turning

r'	0.1	0.2	0.3	0.4
r(rad/s)	0.0222	0.0443	0.0665	0.0887
r'	0.5	0.6	0.7	0.8
r(rad/s)	0.111	0.133	0.155	0.177

Most features of the flow around a ship in oblique flow completely differ from those of a ship moving steadily ahead. The symmetric nature of flow and pressure distribution around the hull becomes extremely asymmetric, yielding a side force and a yaw moment. Figure 4 shows the qualitative distribution of the non-dimensionalized pressure $c_p = (p - p_0)/\frac{1}{2}\rho U^2$ on the hull surface during (a) steady ahead motion and (b) steady ahead/turning combined motion. The stagnation point which was located at the fore front of the bulb has moved to the port side of the bulbous bow, yielding a negative yaw moment. Figure 5 (a) and (b) shows the comparison of absolute fluid velocity distributions on the free surface. Asymmetric flow filed and wake pattern at the stern can be clearly observed at the condition of absolute steady ahead/turning combined motion. Figure 6 shows the relative fluid velocity distribution on the free surface around the vessel. Relative velocity is the one observed from body fixed rotating reference frame. This figure also confirms the exactness of the prescribed motion of vessel, which is combined motion of steady ahead and steady turning "(Hochbaum 2000)". The free stream fluid velocities relative to the body fixed reference frame are as follows:
For steady oblique motion,

$$u = -U\cos\beta, \quad v = -U\sin\beta, \quad w = 0$$

For steady turning motion,

$$u = r \cdot y, \quad v = -r \cdot x, \quad w = 0$$

where U is the advance speed, β is drift angle and r(rad/s) is steady turning rate.

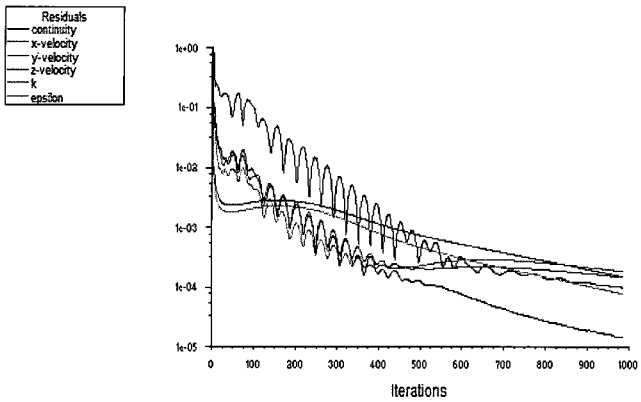

Figure3: History of computation convergence
($U = 1.442 m/s,\ r' = 0.5$)

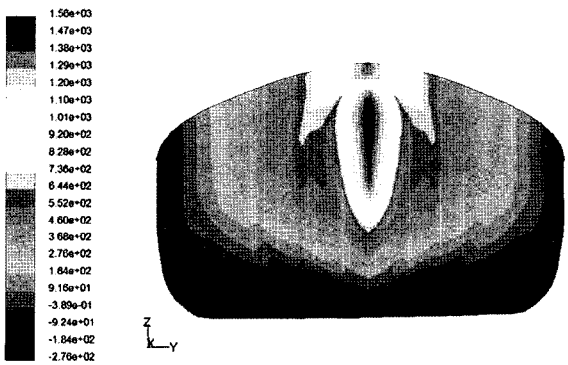

(a) steady ahead motion
($U = 1.442 m/s$)

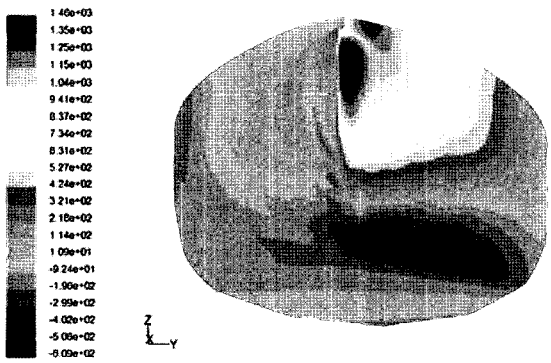

(b) steady ahead/turning combined motion
($U = 1.442 m/s,\ r' = 0.5$)

Figure 4: Pressure distributions on the hull surface

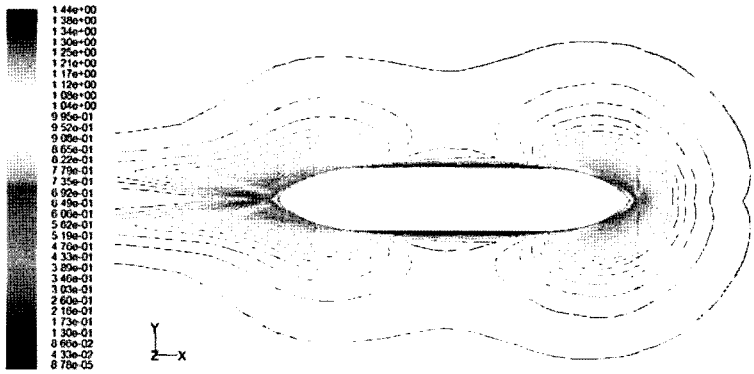

(a) steady ahead motion
($U = 1.442 m/s$)

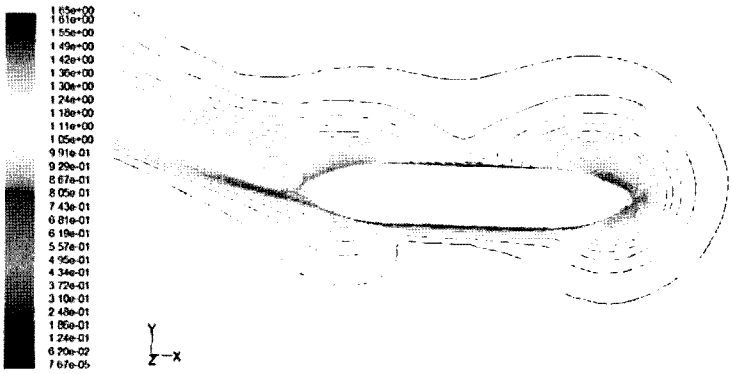

(b) steady ahead/turning combined motion ($U = 1.442 m/s,\ r' = 0.5$)

Figure 5: Absolute velocity contour on the free surface

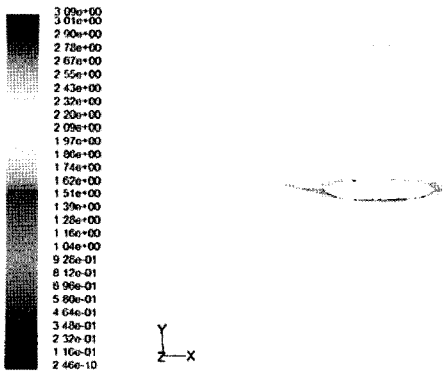

Figure 6: Relative velocity contour on the free surface during steady ahead/turning combined motion ($U = 1.442 m/s,\ r' = 0.5$)

The computed results of hydrodynamic coefficients due to steady oblique motion and steady turning motion are compared with those of MMG Model for scantling draft conditions.

Figure 7 and 8 show the non-dimensionalized side forces, $Y' = Y/\left(\frac{1}{2}\rho L d U^2\right)$, and yaw moments, $N' = N/\left(\frac{1}{2}\rho L^2 d U^2\right)$, respectively, as a function of the non-dimensionalized oblique motion, $v' = v/U$. Comparison is made between the results of CFD calculation and

those of MMG model. The comparison shows generally good qualitative agreement throughout whole range of v' value. But, quantitative difference increases as the magnitude of steady oblique motion increases. It may be premature to make hasty conclusion about which method is better than the other in predicting the hydrodynamic forces in this case. But, MMG model used for the study is empirically introduced based on the database of variety vessels and therefore is subject to unreliable prediction of hydrodynamic forces for a specified vessel.

Figs. 9 and 10 show the non-dimensionalized side forces, $Y' = Y/\left(\frac{1}{2}\rho L d U^2\right)$, and yaw moments, $N' = N/\left(\frac{1}{2}\rho L^2 d U^2\right)$, respectively, as a function of the non-dimensionalized steady turning motion, $r' = r \cdot L/U$. Figure 9 shows noticible difference in the side force prediction varying turning rate. And it must also be notice that the magnitude of coefficient is very small. Figure 10 shows quite good agreement in yaw moment, N' from both methods.

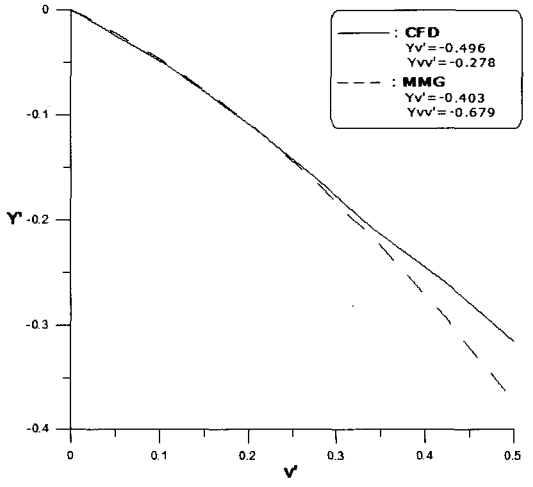

Figure 7: Non-dimensionalized side forces for oblique motion

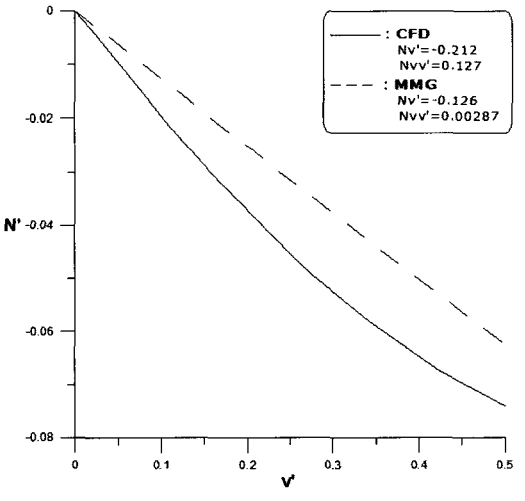

Figure 8: Non-dimensionalized yaw moments for oblique motion

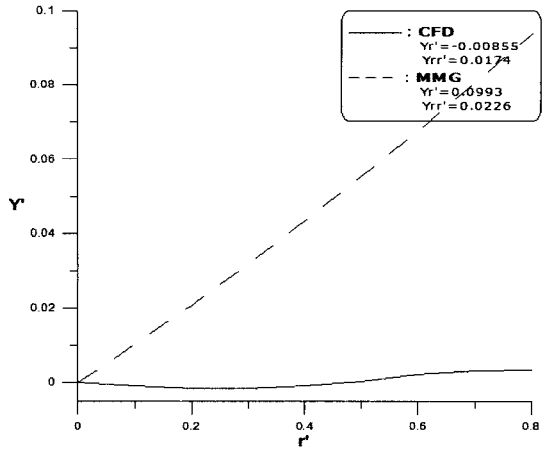

Figure 9: Non-dimensionalized side forces for steady turning motion

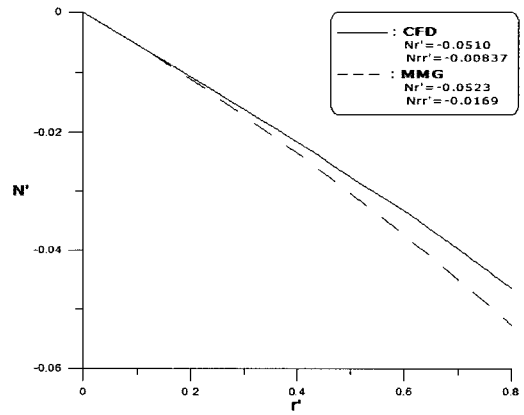

Figure 10: Non-dimensionalized yaw moments for steady turning motion

5 Simulation of manoeuvring motions

The application of RANS based CFD method for the prediction of ship manoeuvrability has been tried by two different approaches. First approach is the indirect CFD based simulation. This method uses one of well developed mathematical models (or MMG models) with hydrodynamic derivatives obtained from CFD application. As mentioned in the previous chapter, present study used this approach. Second approach is the direct CFD based simulation, in which all the hydrodynamic forces due to hull, propeller, rudder and their interactions are provided by CFD analysis for each time step. There is no need for a mathematical model for this approach. This direct simulation technique is still very infant stage to be used for the prediction of ship manoeuvrability even though it will be a useful tool in the future.

In order to confirm the applicability and usefulness of the present approach of indirect CFD based simulation in predicting ship manoeuvrability, standard manoeuvring simulations using three different method, that are CFD, MMG and sea trial, are carried out and the results are compared with each other. Equations (1~6) with equations (13~28) are basic equations and hydrodynamic coefficients used in the MMG simulation. For CFD simulation, basically using same equations as those of MMG model, eight ship motion related hydrodynamic coefficients, which are mentioned and compared in Chapter 4, $Y'_v, N'_v, Y'_{vv}, N'_{vv}, Y'_r, N'_r, Y'_{rr}, N'_{rr}$ are used.

Figure 11 shows the results of 35° standard turning simulations. CFD result gives slightly better agreement with sea trial result than that of MMG. Figs 12 and 13 show the comparisons of 10/10 and 20/20 zig-zag manoeuvres. CFD results show better agreement with sea trial results than those of MMG model.

CFD results show conservative predictions than those of MMG model in both turning simulation and zig-zag manoeuvres; which means larger turning diameter and over shoot angles.

From the simulation results, it is confirmed that the indirect CFD based simulation method used for our study can be used as a reliable and practical prediction tool of ship manoeuvrability.

6 Conclusions

In the present study, the prediction of ship manoeuvrability in the initial design stage has been carried out by use of RANS equation based indirect numerical simulation. Numerically calculated hydrodynamic derivatives are compared with those obtained by MMG model. Standard manoeuvring simulations such as turning circle and zig-zag are also carried out for a medium size Product Carrier and the results are compared with those of MMG model and manoeuvring sea trial. Following conclusions are made.

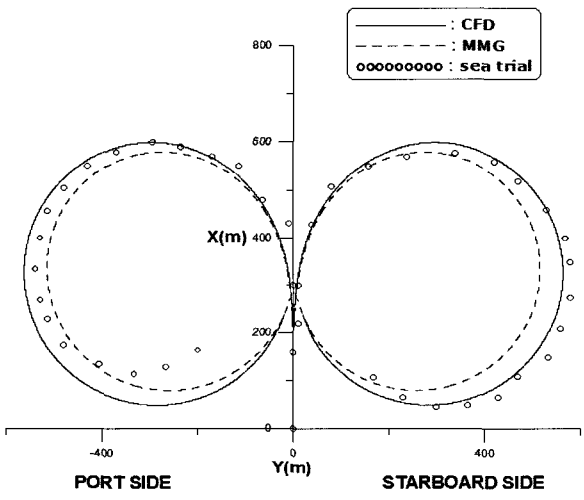

Figure 11: Comparison of turning manoeuvre (CFD, MMG, Sea trial)

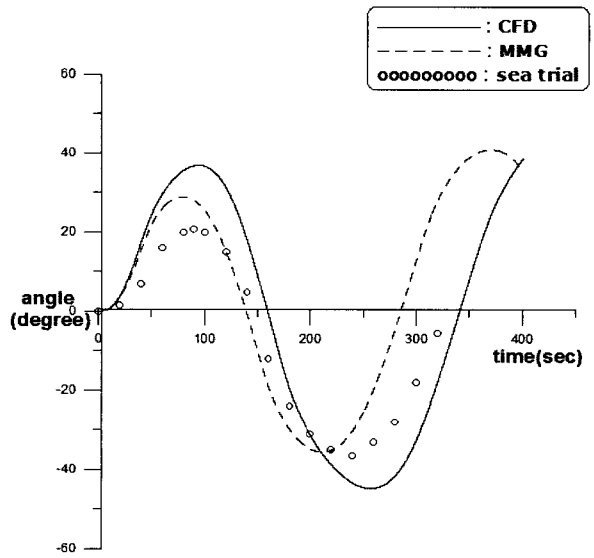

Figure 12: Comparison of 10/10 zig-zag manoeuvres (CFD, MMG, Sea trial)

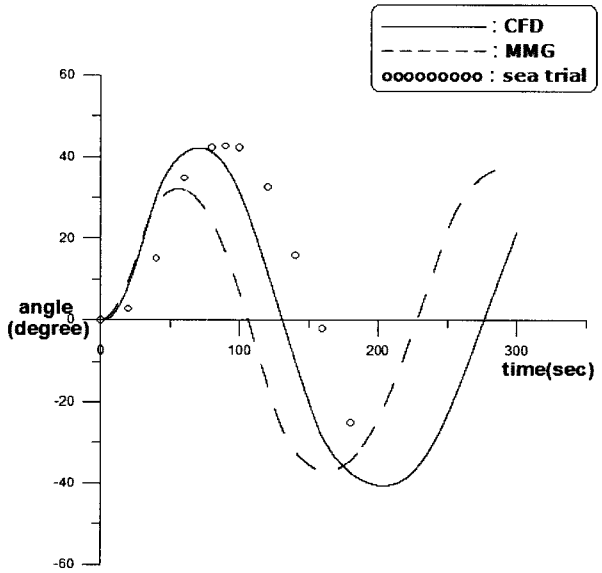

Figure 13: Comparison of 20/20 zig-zag manoeuvres (CFD, MMG, Sea trial)

(1) An indirect CFD based simulation method using well known MMG models and commercial CFD code 'Fluent' is successfully applied for the prediction of ship manoeuvrability

(2) Generally good qualitative agreement is obtained in hydrodynamic forces to manoeuvring vessel during steady oblique and steady turning motions between the results of CFD calculation and those of MMG model.

(3) Standard manoeuvring simulation results show that the indirect CFD based simulation

method can be used as a practical prediction tool for ship manoeuvrability.
(4) Validation of CFD results related to the hull form modeling, grid generation, treatments of boundary conditions, turbulence modeling, and comparison with experimental results are still subject to further studies for the prediction of ship manoeuvrability.

Acknowledgements

The authors would like to express deep appreciation to Hyundai Mipo Dockyard for financial support of the present research.

References

FLUENT. 2003. Ver. 6.1.22 User manual.

Fujino, M. 1996. Prediction of Ship. Manoeuvrability : State of Art, MARSIM '96, 371-387.

Hochbaum, A.C. 2000. Computation of the Turbulent Flow Around a Ship Model in Steady Turn and in Steady Oblique Motion, 22nd Symp. on Naval Hydrodynamics, 550-567.

IMO. 2002. Standards for Ship Manoeuvrability Resolution MSC.137(76), December, 2002.

Inoue, S., M. Hirano and K. Kijima. 1981. Hydrodynamic Derivatives on Ship Manoeuvring, ISP, **28, 321.**

Kijima, K., T. Katsumo, Y. Nakiri and Y. Furukawa. 1990. On the Manoeuvring Performance of a Ship with the Parameter of Loading Condition, J. of SNAJ, **168.**

Kim, S.-Y. and Y.-G. Kim. 2001. Computation of Viscous Flows around a Ship with a Drift Angle and Effects of Stern Hull Form on the Hydrodynamic Forces, J. of SNAK, **38, 3,** 1-13.

Lee, S.-W, H. Lee, E.-S. Jin, S.-Y. Kim and Y.-K. Kim. 2004. Prediction of Manoeuvrability of Big Container Ship by CFD, Proc. 45th W/S of KTTC, 25-32.

Ohmori, T. and H. Miyata. 1993. Oblique Tow Simulation by a Finite Volume Method, J. of SNAJ, **173,** 27-34.

Tahara, Y., J. Longo, F. Stern and Y. Himeno. 2002. Comparison of CFD and EFD for the Series 60 CB=0.6 in Steady Yaw Motion, 22nd Symp. on Naval Hydrodynamics, 981-998.